

The cosmological implications of massive, high-redshift galaxy clusters.

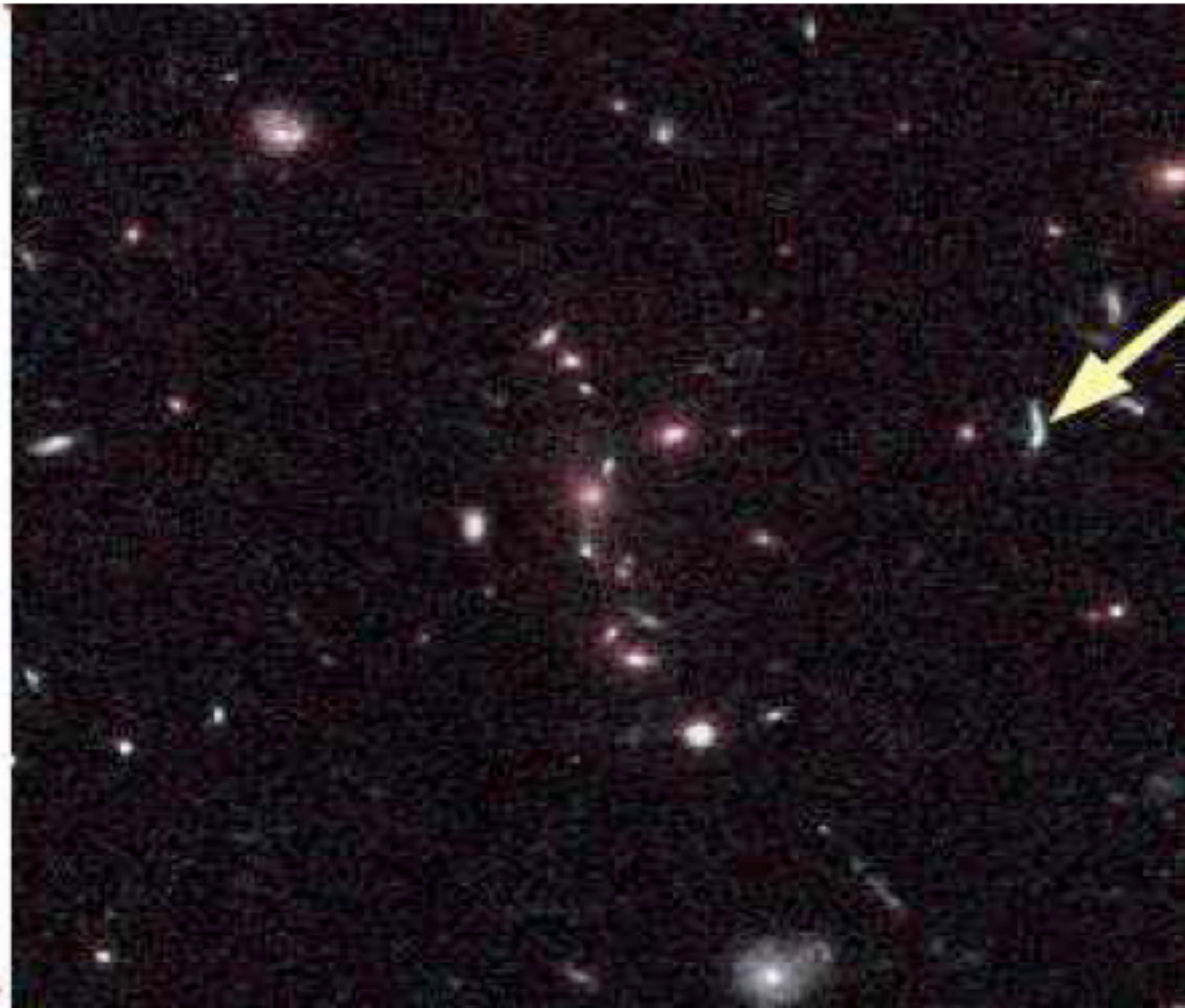
**Ben Hoyle, Raul Jimenez, Licia Verde, ICC-IEEC University of Barcelona,
University of Helsinki: Hoyle et al 2011 (+ in prep)**

Overview

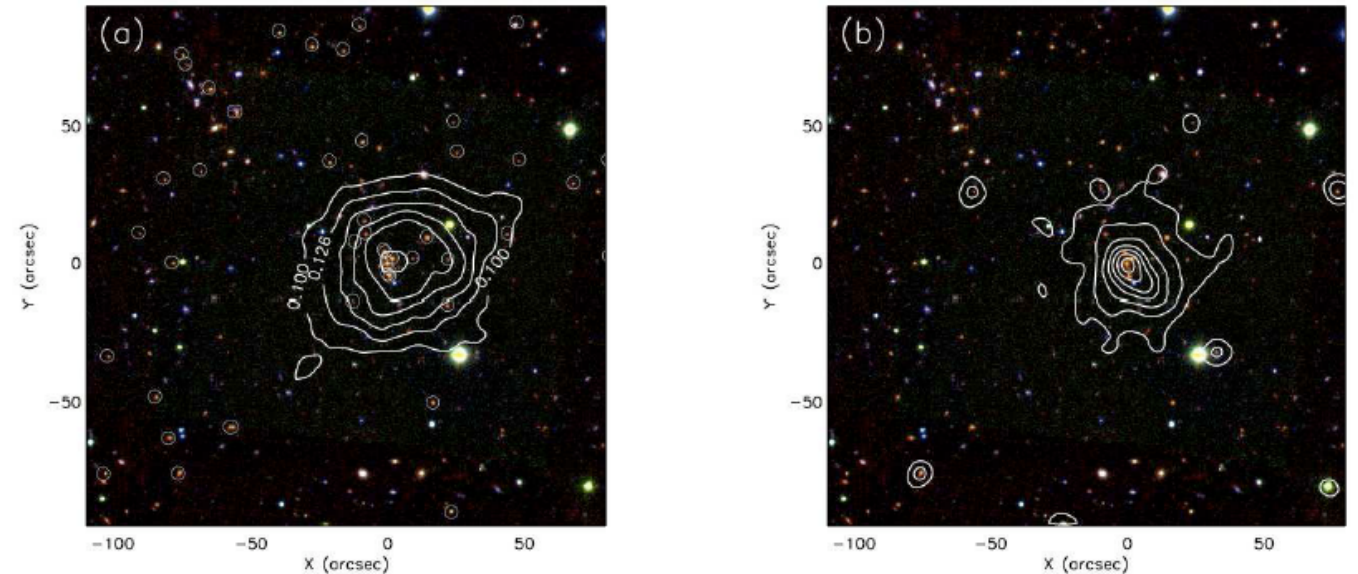
- **Observational motivation**
- **Theory**
- **The cluster sample**
- **The XMM Cluster Survey**
- **Analysis and Results**
- **Possible explanations: Systematics**
- **Other work**
- **New Analysis and Results**
- **Conclusions**

Motivation: observations of XMMJ2235

Some recent observations have called into question some of the underlying assumptions of the Λ CDM model + WMAP priors on the cosmological parameters. E.g., A very massive clusters of galaxies at high redshift, was statistically unlikely to have been observed.



Jee et al 2009



$$M_{200} = 7.7 \pm 1.3 \times 10^{14} M_{\odot}$$

$$M_{200} = 7.7^{+4.4}_{-3.3} \times 10^{14} M_{\odot}$$

$$z = 1.4$$

How likely was this cluster to be observed?

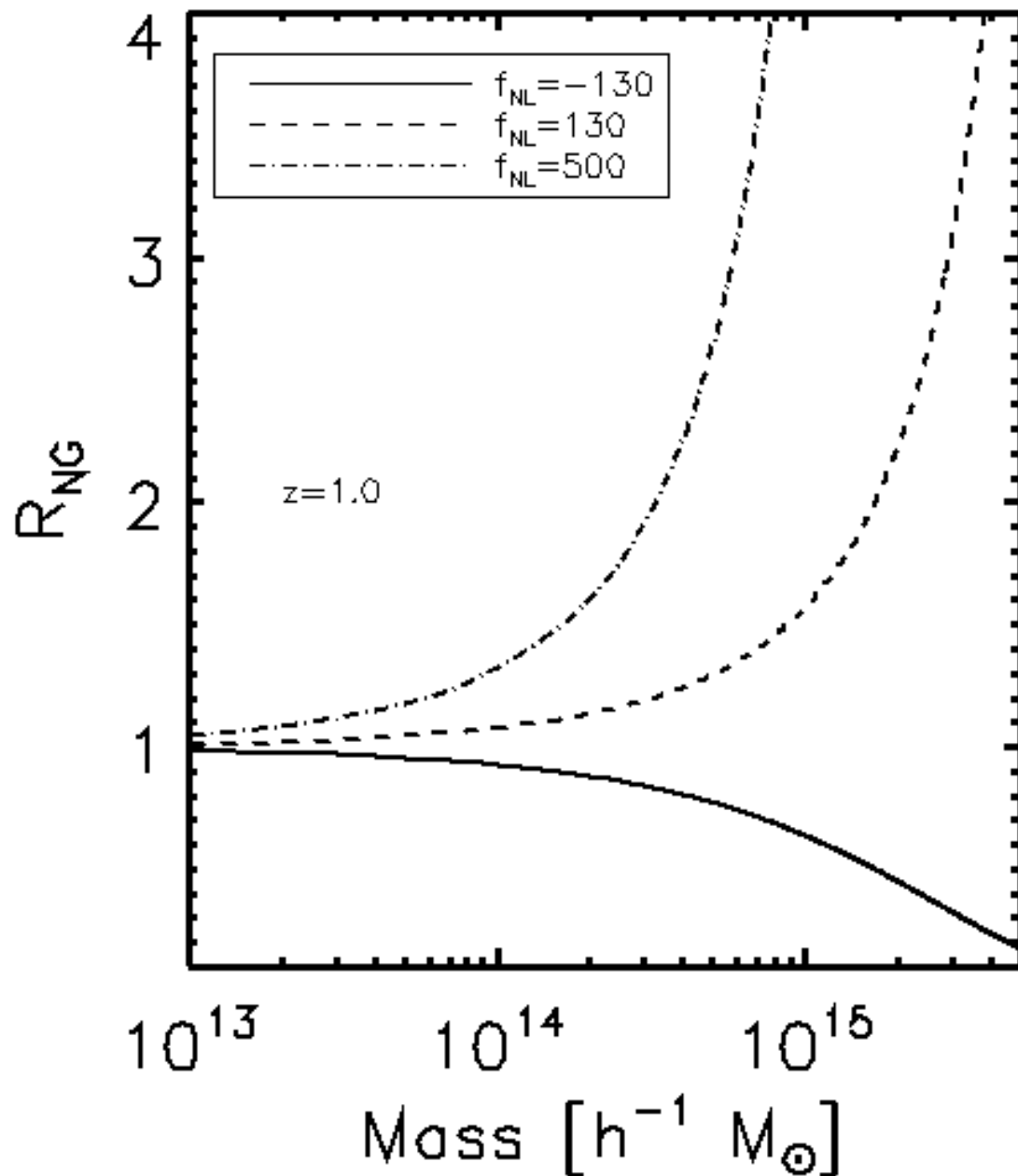
- The expected number in the full sky ~ 7 .
- Footprint was 11 square degrees XMM X-ray survey, 0.02% of sky.
- Poisson sample from $(0.0002 \times 7) > 1$ only 1.4%

Jimenez & Verde 2009 showed values of $f_{nl} \sim 150$ relieves tension with XMM J2235.

Motivation: theory, a window to the early Universe

Using today's data, (not some future experiment e.g. LISA-like) we can make a measurement of the amount of primordial non-Gaussianity (f_{NL}) of the initial density perturbations, which can tell us about the various types of scalar field interactions during inflation/reheating/preheating.

Byrnes et al 2010 [arXiv:1007.4277]



$$\Phi = \phi + f_{\text{NL}} (\phi^2 - \langle \phi^2 \rangle) .$$

$$\mathcal{R}_{\text{NG}}(S_{3,M}, M, z) = \frac{n(M, z, f_{\text{NL}})}{n_G(M, z, f_{\text{NL}} = 0)}$$

Solved in the Press-Schechter type formalism by Matarrese, Verde, Jimenez 2002, LoVerde et al 2007, Maggiore et al 2009, D'Amico et al 2010 etc.

Rng enable other, better calibrated mass functions to be used (e.g., Jenkins et al 2000, Tinker et al 2008, Wagner et al 2010).

Motivation: observations II - More massive clusters

SPT CL J0546-5345

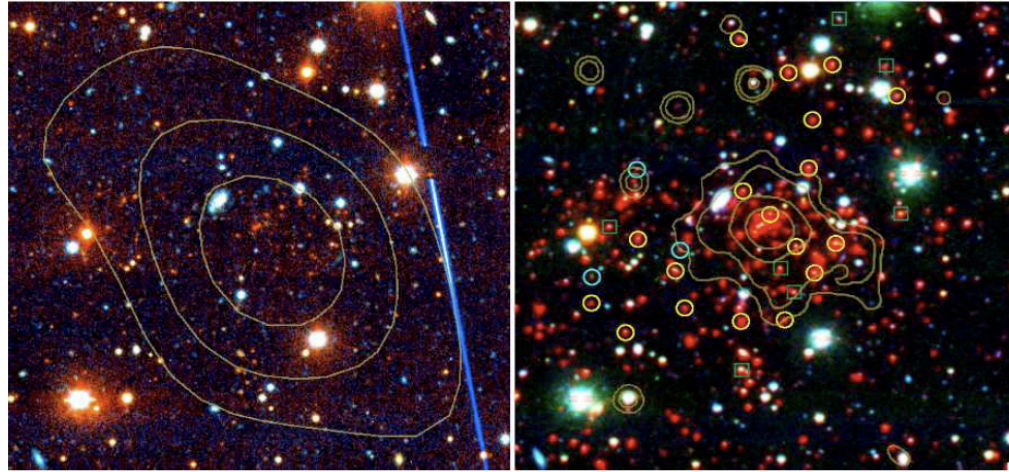


FIG. 1.— *Left*: Optical $4' \times 4'$ color image (*grz*) of SPT-CL J0546-5345, with SZE significance contours overlaid ($S/N = 2, 4,$ and 6). *Right*: False color optical (*ri*) + IRAC ($3.6 \mu\text{m}$) image of SPT-CL J0546-5345, with *Chandra* X-ray contours overlaid ($0.25, 0.4, 0.85$ and 1.6 counts per $2'' \times 2''$ pixel per 55.6 ks in the $0.5\text{-}2$ keV band). North is up, east is to the left. Due to its high angular resolution, *Chandra* is able to resolve substructure to the SW, which may be evidence of a possible merger. These images highlight the importance of IRAC imaging in studying the galaxies in high redshift, optically faint clusters. Spectroscopic early-type (late-type) members are indicated with yellow (cyan) circles. Green squares show the spectroscopic non-members.

$$M_{200} \sim 10^{15} M_{\odot}! \quad z = 1.05$$

- Expect to see one 18% of time

Brodwin et al 2010

SPT-CL J2106-5844

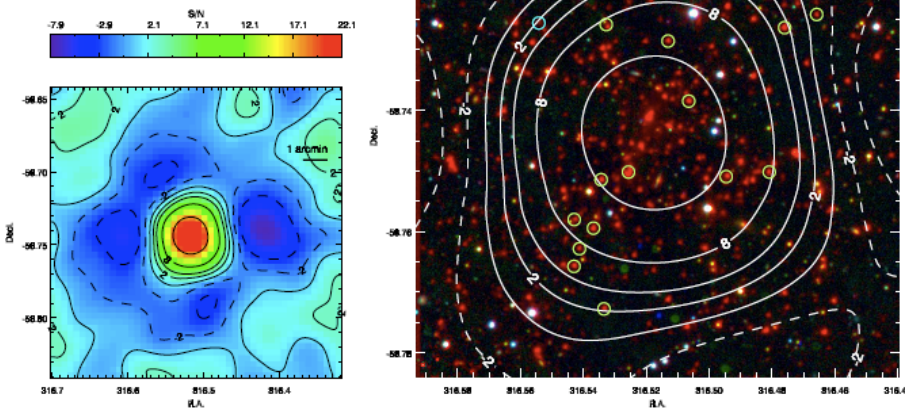
$$M_{200} = 1.27 \times 10^{15} h^{-1} M_{\odot}!$$

$$z = 1.13$$

- Expect to see one 5.9% of time

Foley et al 2011

Foley et al.



More clusters.

Are these clusters consistent with LCDM?

B.H., Jimenez, Verde 2010, See also Mortonson et al 2010, Enqvist, Hotchkiss, Taanila 2011, Hotchkiss 2011, B.H. et al in prep.

- **Spectroscopic redshifts > 1**
- **3 SZ detected**
- **11 X-ray detected**

Cluster Name	Redshift	M_{200}	$10^{14} M_{\odot}$	Method
'WARPSJ1415.1+3612' +	1.02	$3.33^{+2.83}_{-1.80}$	Velocity dispersion	
'SPT-CLJ2341-5119' *	1.03	$7.60^{+3.94}_{-3.94}$	Richness	
'XLSSJ022403.9-041328' +	1.05	$1.66^{+1.15}_{-0.38}$	X-ray	
→'SPT-CLJ0546-5345' *	1.06	$10.0^{+6.00}_{-4.00}$	Velocity dispersion	
'SPT-CLJ2342-5411' *	1.08	$4.08^{+2.53}_{-2.53}$	Richness	
'RDCSJ0910+5422' +	1.10	$6.28^{+3.70}_{-3.70}$	X-ray	
'RXJ1053.7+5735(West)' +	1.14	$2.00^{+1.00}_{-0.70}$	X-ray	
'XLSSJ022303.0043622' +	1.22	$1.10^{+0.60}_{-0.40}$	X-ray	
'RDCSJ1252.9-2927' +	1.23	$2.00^{+0.50}_{-0.50}$	X-ray	
'RXJ0849+4452' +	1.26	$3.70^{+1.90}_{-1.90}$	X-ray	
'RXJ0848+4453' +	1.27	$1.80^{+1.20}_{-1.20}$	X-ray	
→'XMMUJ2235.3+2557' +	1.39	$7.70^{+4.40}_{-3.10}$	X-ray	
'XMMXCSJ2215.9-1738' +	1.46	$4.10^{+3.40}_{-1.70}$	X-ray	
'SXDF-XCLJ0218-0510' +	1.62	$0.57^{+0.14}_{-0.14}$	X-ray	

The next generation of cluster samples will be found by X-ray (eRosita ~ 100,000) not SZ (ActPol ~ 1000). All X-ray clusters detected or redetected with XMM Cluster Survey

XCS:

XMM Cluster Survey

Members: Kathy Romer [P.I], John P. Stott, Claire Burke, E. J. Lloyd-Davies, Mark Hosmer, Nicola Mehrtens, Michael Davidson, Kivanc Sabirli, Robert G. Mann, **Matt Hilton, Andrew R. Liddle, Pedro T. P. Viana, Heather C. Campbell, Chris A. Collins, E. Naomi Dubois, Peter Freeman, Ben Hoyle, **Scott T. Kay**, Emma Kuwertz, Christopher J. Miller, Robert C. Nichol, Martin Sahlen, S. Adam Stanford.**

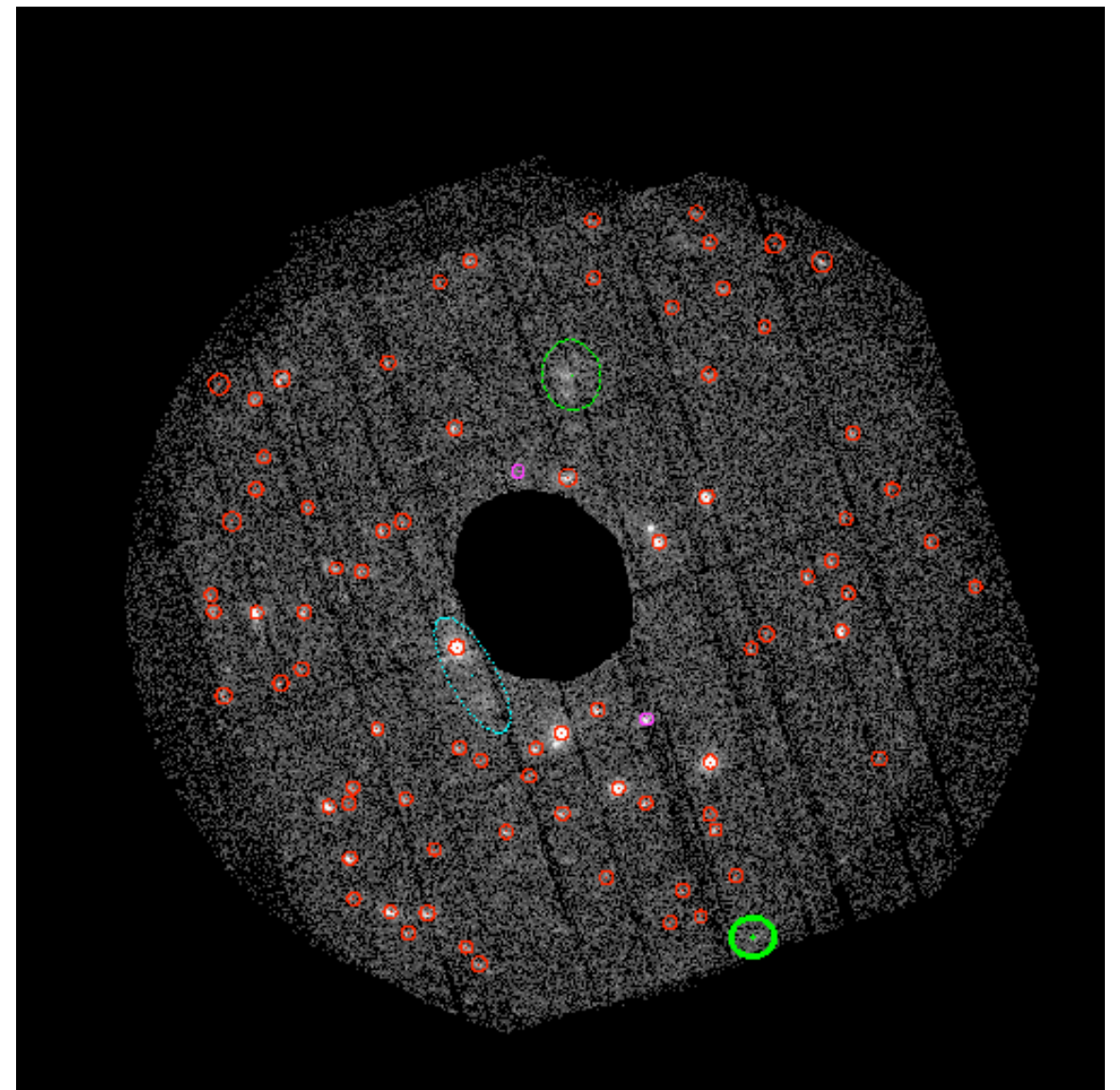
- **The XMM Cluster Survey aims to mine the XMM science archive for galaxy clusters**

X-ray emission is the smoking gun, but it's not enough. Need optical identification and redshifts (X-ray redshift difficult) before the fluxes can be converted to temperatures and masses.

Algorithms paper, Lloyd-Davies et al. 2010 (arXiv:1010.0677)

See Matt's talk for all the juicy details.

**Recent data release,
Mehrtens et al. arXiv:1106.3056
503 clusters, spanning $0.06 < z < 1.46$
438 have x-ray temperatures**



More Clusters. Data sample

Cluster Name	Redshift	M_{200} $10^{14}M_{\odot}$	Method
'WARPSJ1415.1+3612' +	1.02	$3.33^{+2.83}_{-1.80}$	Velocity dispersion
'SPT-CLJ2341-5119' *	1.03	$7.60^{+3.94}_{-3.94}$	Richness
'XLSSJ022403.9-041328' +	1.05	$1.66^{+1.15}_{-0.38}$	X-ray
→'SPT-CLJ0546-5345' *	1.06	$10.0^{+6.00}_{-4.00}$	Velocity dispersion
'SPT-CLJ2342-5411' *	1.08	$4.08^{+2.53}_{-2.53}$	Richness
'RDCSJ0910+5422' +	1.10	$6.28^{+3.70}_{-3.70}$	X-ray
'RXJ1053.7+5735(West)' +	1.14	$2.00^{+1.00}_{-0.70}$	X-ray
'XLSSJ022303.0043622' +	1.22	$1.10^{+0.60}_{-0.40}$	X-ray
'RDCSJ1252.9-2927' +	1.23	$2.00^{+0.50}_{-0.50}$	X-ray
'RXJ0849+4452' +	1.26	$3.70^{+1.90}_{-1.90}$	X-ray
'RXJ0848+4453' +	1.27	$1.80^{+1.20}_{-1.20}$	X-ray
→'XMMUJ2235.3+2557' +	1.39	$7.70^{+4.40}_{-3.10}$	X-ray
'XMMXCSJ2215.9-1738' +	1.46	$4.10^{+3.40}_{-1.70}$	X-ray
'SXDF-XCLJ0218-0510' +	1.62	$0.57^{+0.14}_{-0.14}$	X-ray

Conservative assumptions

Footprints; If there was overlap between the surveys, we conservatively assumed each X-ray survey had it's own unique footprint

- **Survey volumes: We assumed all surveys had the redshift depth of the deepest survey $z \sim 2.2$**
- **Selection functions: For each cluster, we assumed that any similar ($>M$) cluster at any higher redshift would have been detected.**
- **Mass estimates: We chose to use the cluster mass and error which gave the least tension with LCDM**

Analysis & Results I

For each cluster “i”, we sample S , from the mass and error 10,000 times. We calculate the expected abundance of clusters above each sampled mass and redshift using the theoretical cluster mass function.

$$A_s = \int_{M_s}^{\infty} \int_{z=z_{cluster}}^{z=2.2} n(m, z, f_{NL}, C) dm dz$$

We Poisson sample P^O , from the expected abundance (A_s) for this realisation.

If the Poisson sample is >1 , the cluster exists in this realisation.

If the Poisson sample is <1 the cluster does not exist in this realisation.

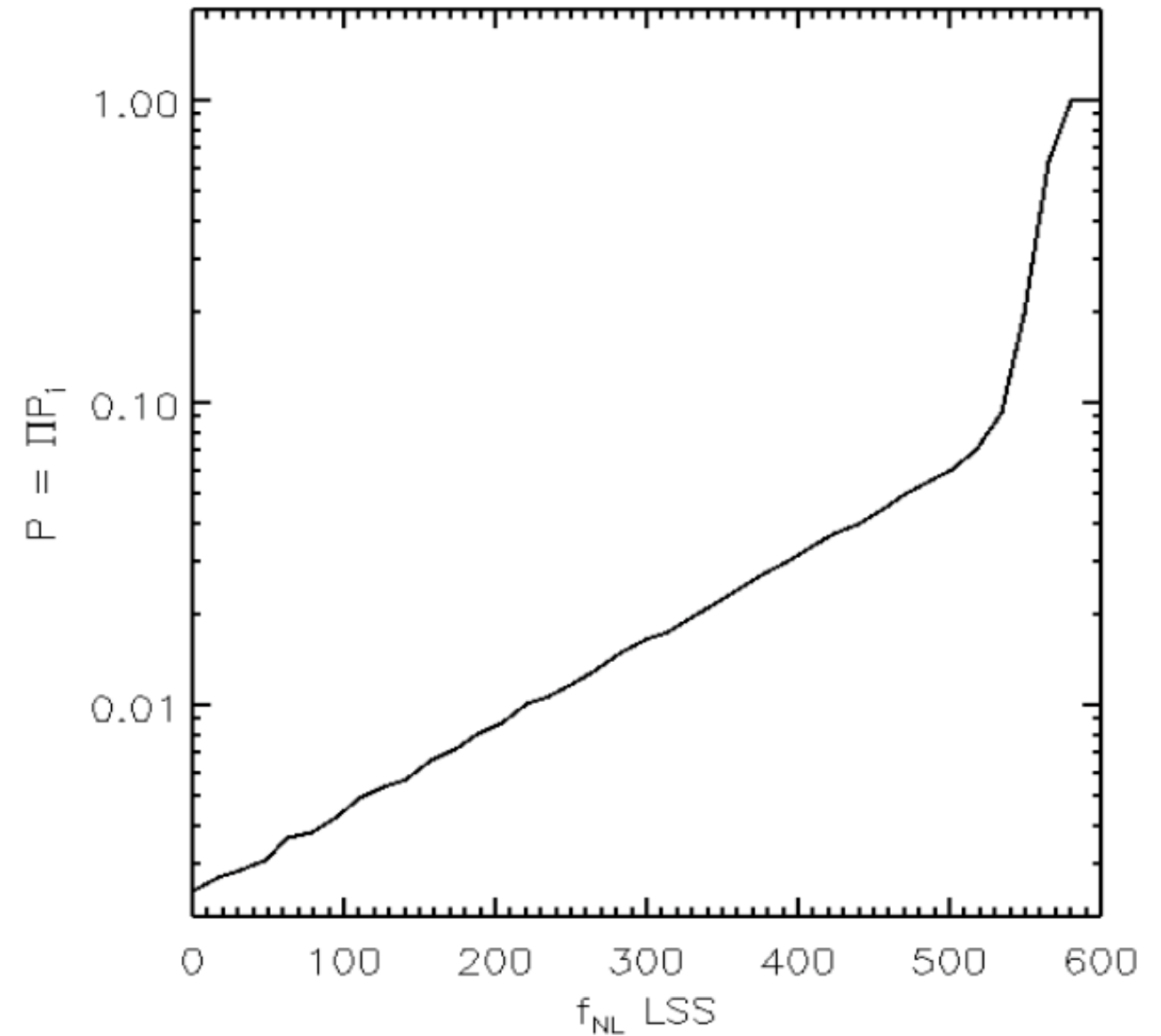
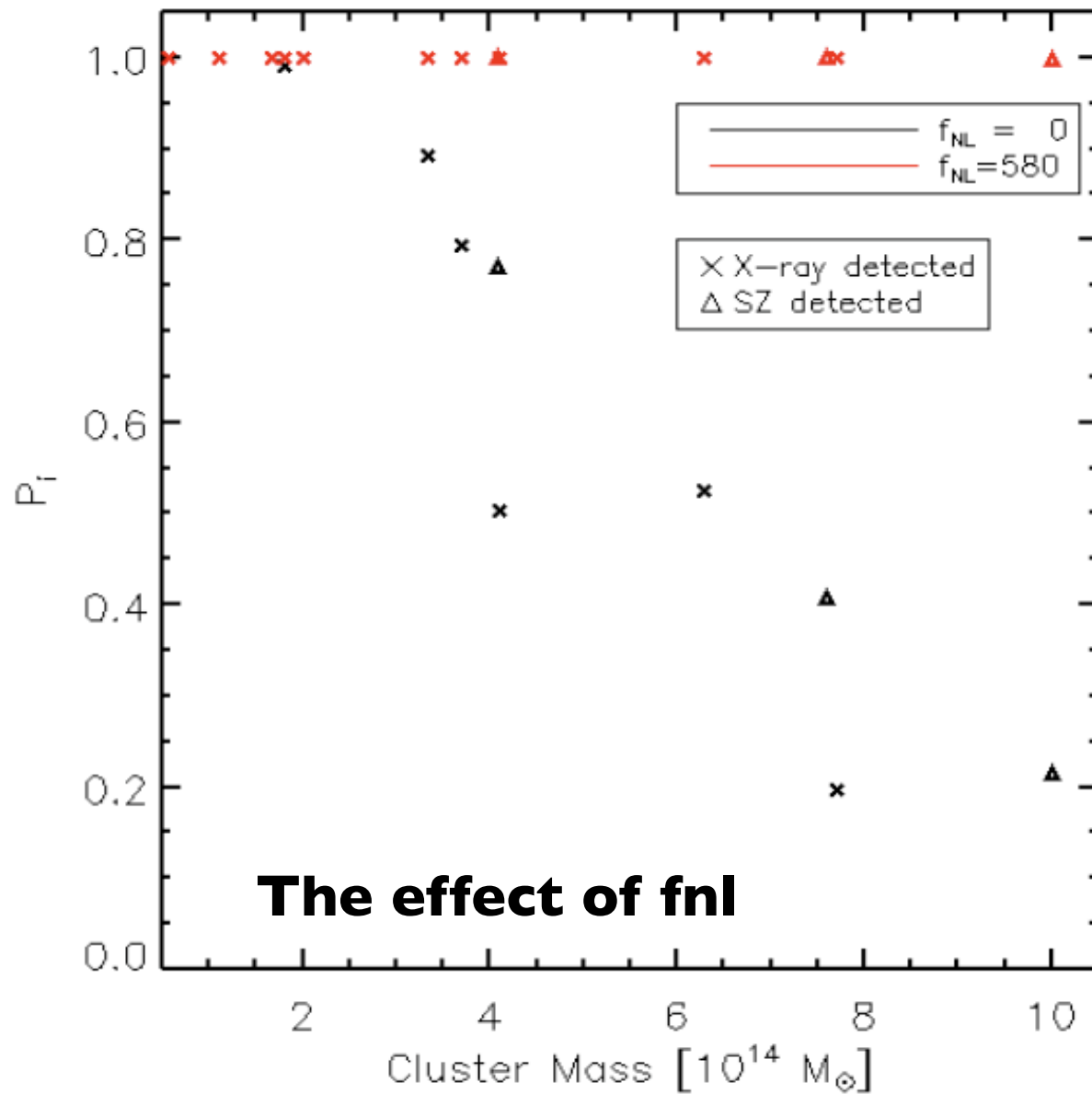
The probability P_i , that cluster “i” exists is $\text{Number}(P^O(A_s) \geq 1)/10^4$

The probability, that the ensemble of cluster exists is $P(f_{NL}, C) = \prod P_i$

We multiply the probabilities, because the clusters are typically separated by vast redshifts, and positions on the sky. We therefore model them as being independent events.

Analysis & Results I

Fixed cosmological parameters to best fit WMAP 5

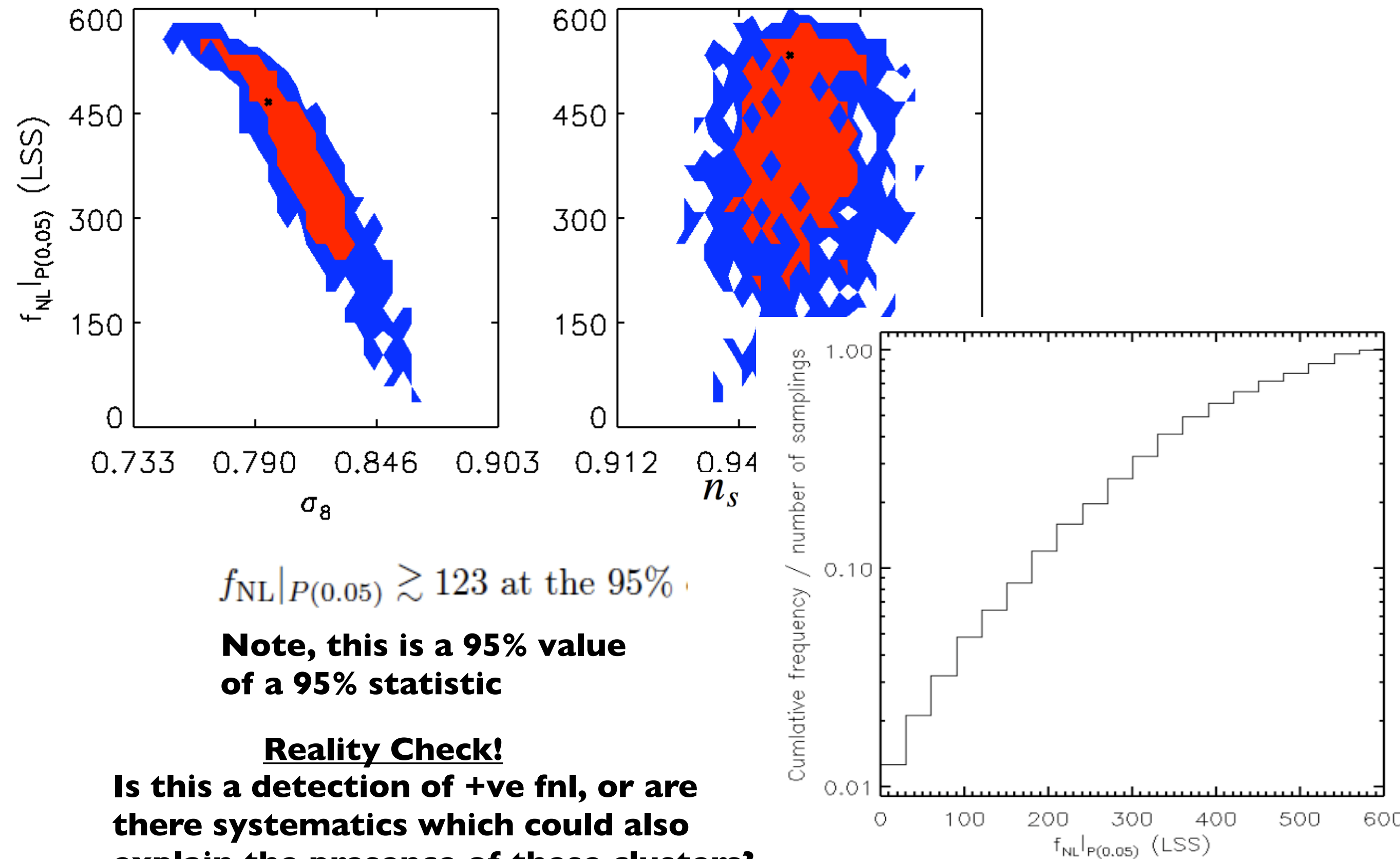


We determine the value of f_{NL} where P=0.05
i.e., the value of f_{NL} that contains 95% of the probability $f_{NL} |_{P(0.05)}$

At the 95% confidence level, $f_{NL} > 467$

Analysis & Results I

Marginalising over parameters; $\Omega_M, \Omega_b, \Omega_\Lambda, \Omega_K, n_s, \sigma_8, H_0, w_0$



$f_{\text{NL}}|_{P(0.05)} \gtrsim 123$ at the 95%

**Note, this is a 95% value
of a 95% statistic**

Reality Check!

**Is this a detection of +ve fnl, or are
there systematics which could also
explain the presence of these clusters?**

Possible explanations: Systematics

I) Cosmological parameters.

- **If $\sigma_8 = 0.9$ tension is removed.**
- **But CMB + LSS find (Komatsu et al 2011)**

$$\sigma_8 = 0.801 \pm 0.03$$

Possible explanations: Systematics

1) Cosmological parameters.

- **If $\sigma_8 = 0.9$ tension is removed.**
- **But CMB + LSS find (Komatsu et al 2011)**

$$\sigma_8 = 0.801 \pm 0.03$$

2) Mass functions.

Do we understand the mass function (with fnl, e.g., Tinker) at high mass and redshift well enough?

Possible explanations: Systematics

1) Cosmological parameters.

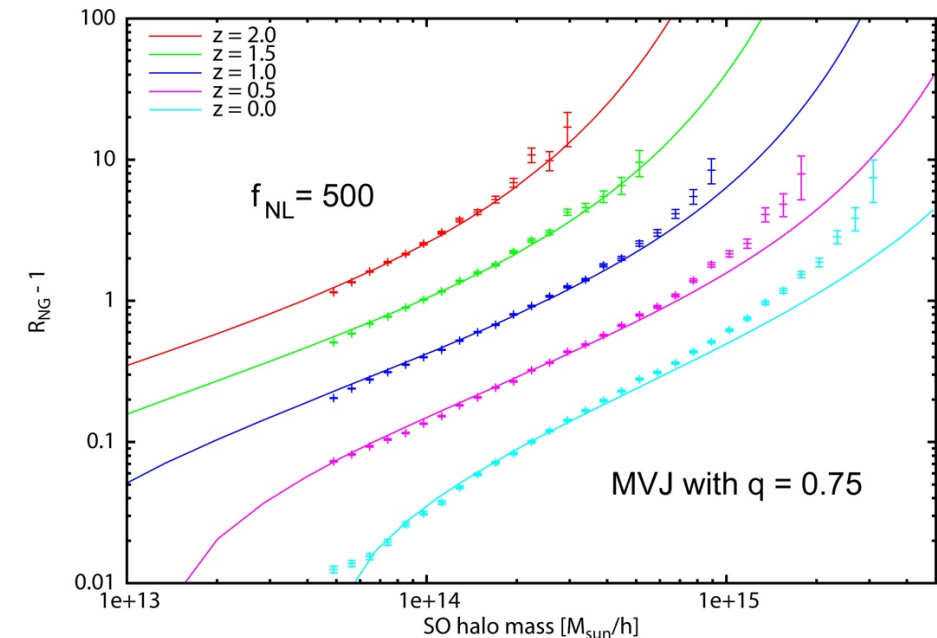
- If $\sigma_8 = 0.9$ tension is removed.
- But CMB + LSS find (Komatsu et al 2011)

$$\sigma_8 = 0.801 \pm 0.03$$

2) Mass functions.

Do we understand the mass function (with f_{NL}, e.g., Tinker) at high mass and redshift well enough?

-- Yes new simulation work by Christian Wagner f_{NL}<500, z<1.5, M<5x10¹⁴ Msol



Non-Gaussian mass function fit to N-body simulations

Volume: $40 \times (2.4 \text{ Gpc}/h)^3$

Number of Particles: 40×768^3

Spherical-overdensity halos with "virial" masses

Difference for very large halo masses might be due to f_{NL}^2 effects.

Possible explanations: Systematics

1) Cosmological parameters.

- **If $\sigma_8 = 0.9$ tension is removed.**
- **But CMB + LSS find (Komatsu et al 2011)**

$$\sigma_8 = 0.801 \pm 0.03$$

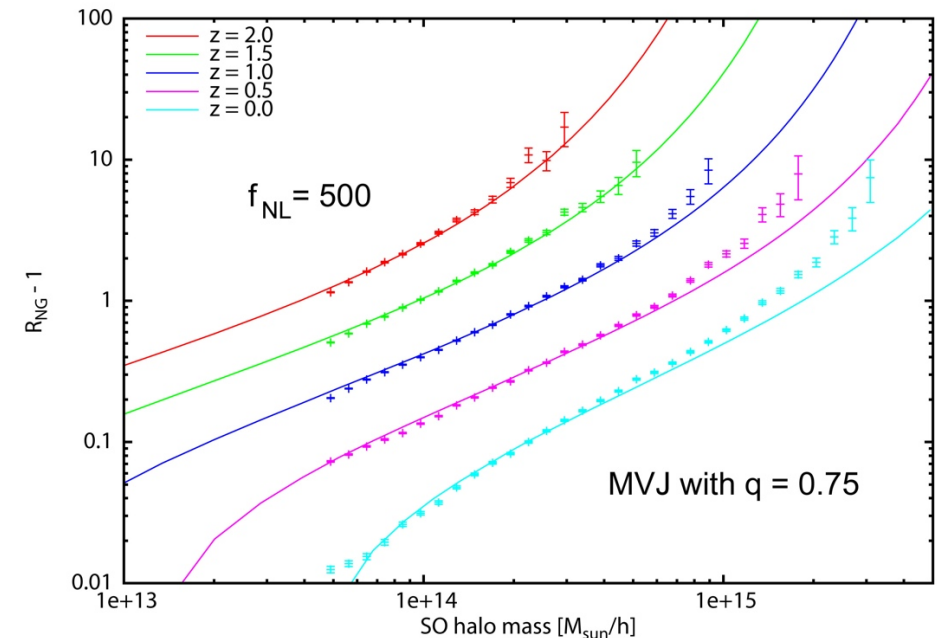
2) Mass functions.

Do we understand the mass function (with f_{NL}, e.g., Tinker) at high mass and redshift well enough?

--Yes new simulation work by Christian Wagner f_{NL}<500, z<1.5, M<5x10¹⁴ Msol

3) Mass measurements.

If every mass measurement was 1.5 sigma higher than the “true” value, then all tension is relieved. But all independent mass estimates must be systematically, equally wrong.



Non-Gaussian mass function fit to N-body simulations

Volume: 40 x (2.4 Gpc/h)³

Number of Particles: 40 x 768³

Spherical-overdensity halos with “virial” masses

Difference for very large halo masses might be due to f_{NL}² effects.

Possible explanations: Systematics

1) Cosmological parameters.

- If $\sigma_8 = 0.9$ tension is removed.
- But CMB + LSS find (Komatsu et al 2011)
 $\sigma_8 = 0.801 \pm 0.03$

2) Mass functions.

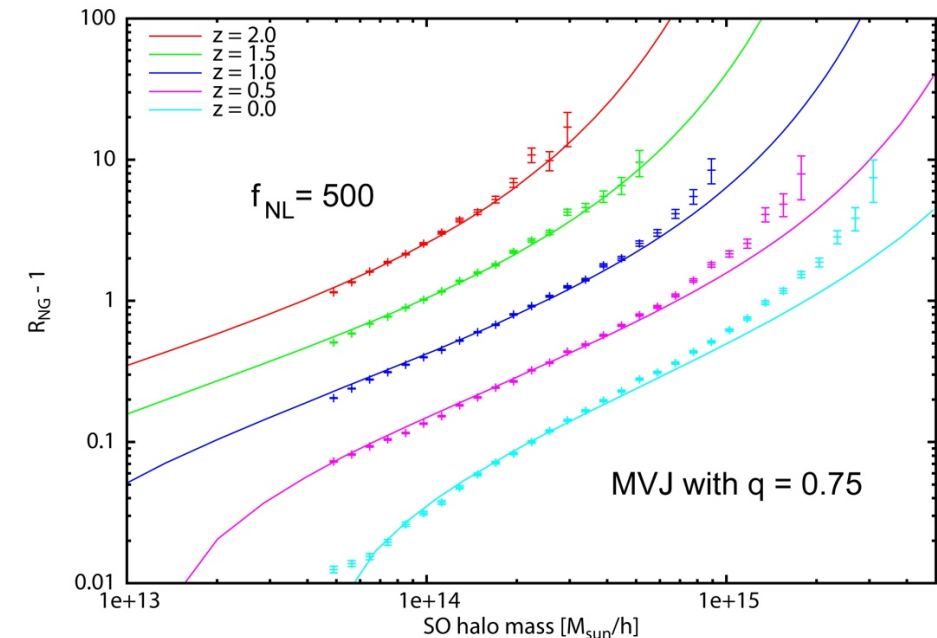
Do we understand the mass function (with f_{NL}, e.g., Tinker) at high mass and redshift well enough?

-- Yes new simulation work by Christian Wagner f_{NL}<500, z<1.5, M<5x10¹⁴ Msol

3) Mass measurements.

If every mass measurement was 1.5 sigma higher than the “true” value, then all tension is relieved. But all independent mass estimates must be systematically, equally wrong.

Failed HST WL proposal :([PI BH].



Non-Gaussian mass function fit to N-body simulations

Volume: $40 \times (2.4 \text{ Gpc}/h)^3$

Number of Particles: 40×768^3

Spherical-overdensity halos with "virial" masses

Difference for very large halo masses might be due to f_{NL}^2 effects.

Possible explanations: Systematics

1) Cosmological parameters.

- If $\sigma_8 = 0.9$ tension is removed.
- But CMB + LSS find (Komatsu et al. 2011)

$$\sigma_8 = 0.801 \pm 0.03$$

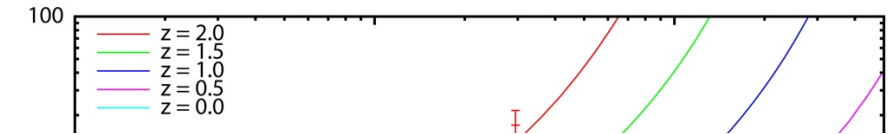
2) Mass functions.

Do we understand the mass function (with fnl, e.g., Tinker) at high redshift well enough?

-- Yes new simulation work by Wagner et al. (2015) fnl < 500, z < 1.5, M < 5 x 10^14 M_sun

3) Mass measurements.

If every mass measurement was sigma higher than the "true" value, all tension is relieved. But all independent mass estimates are systematically, equally wrong.



Cluster Name	Redshift	M_{200}	$10^{14} M_{\odot}$	Method	Footprint	Mass reference
RCS0221-0321	1.02	$1.80^{+1.30}_{-0.70}$		WL	100.	[16]
RCS0220-0333	1.03	$4.80^{+1.80}_{-1.30}$		WL	100.	[16]
WARPSJ1415+3612	1.03	$4.70^{+2.00}_{-1.40}$		WL	100.	[16]
RCS2345-3632	1.04	$2.40^{+1.10}_{-0.70}$		WL	100.	[16]
XLSSJ022403.9-041328	1.05	$1.66^{+1.15}_{-0.38}$		X-ray	100.	[30]
RCS2156-0448	1.07	$1.80^{+2.50}_{-1.00}$		WL	100.	[16]
RCS0337-2844	1.10	$4.90^{+2.80}_{-1.70}$		WL	100.	[16]
ISCSJ1432+3332	1.11	$4.90^{+1.60}_{-1.20}$		WL	100.	[16]
RDCSJ0910+5422	1.11	$5.00^{+1.20}_{-1.00}$		WL	100.	[16]
XMMUJ2205-0159	1.12	$3.00^{+1.60}_{-1.00}$		WL	100.	[16]
RXJ1053.7+5735(West)	1.14	$2.00^{+1.00}_{-0.69}$		X-ray	100.	[30]
XLSSJ0223-0436	1.22	$7.40^{+2.50}_{-1.80}$		WL	100.	[16]
RDCSJ1252-2927	1.24	$6.80^{+1.20}_{-1.00}$		WL	100.	[16]
ISCSJ1434+3427	1.24	$2.50^{+2.20}_{-1.10}$		WL	100.	[16]
ISCSJ1429+3437	1.26	$5.40^{+2.40}_{-1.60}$		WL	100.	[16]
RDCSJ0849+4452	1.26	$4.40^{+1.10}_{-0.90}$		WL	100.	[16]
RDCSJ0848+4453	1.27	$3.10^{+1.00}_{-0.80}$		WL	100.	[16]
ISCSJ1432+3436	1.35	$5.30^{+2.60}_{-1.70}$		WL	100.	[16]
ISCSJ1434+3519	1.37	$2.80^{+2.90}_{-1.40}$		WL	100.	[16]
XMMUJ2235-2557	1.39	$7.30^{+1.70}_{-1.40}$		WL	100.	[16]
ISCSJ1438+3414	1.41	$3.10^{+2.60}_{-1.40}$		WL	100.	[16]
XMMXCSJ2215-1738	1.46	$4.30^{+3.00}_{-1.70}$		WL	100.	[16]
SPT-CLJ2341-5119	1.03	$7.60^{+3.94}_{-3.94}$		SZ	2500	[1]
SPT-CLJ2342-5411	1.08	$4.08^{+2.53}_{-2.53}$		SZ	2500	[1]
SPT-CLJ0546-5345	1.06	$7.95^{+0.92}_{-0.92}$		Mixed	2500	[3]
SPT-CLJ2106-5844	1.13	$12.7^{+2.10}_{-2.10}$		SZ	2500	[10]

Failed HST WL proposal :([PI BH].

Jee et al 2011

- Gurvan Basin HST WL.

Related works

Mortonson et al 2010

- Treatment of the Eddington bias
- Tension curve for I cluster.

- Very conservative footprints and mass estimates.
- Insensitive treatment of multiple clusters
- Caution using this if know SF.

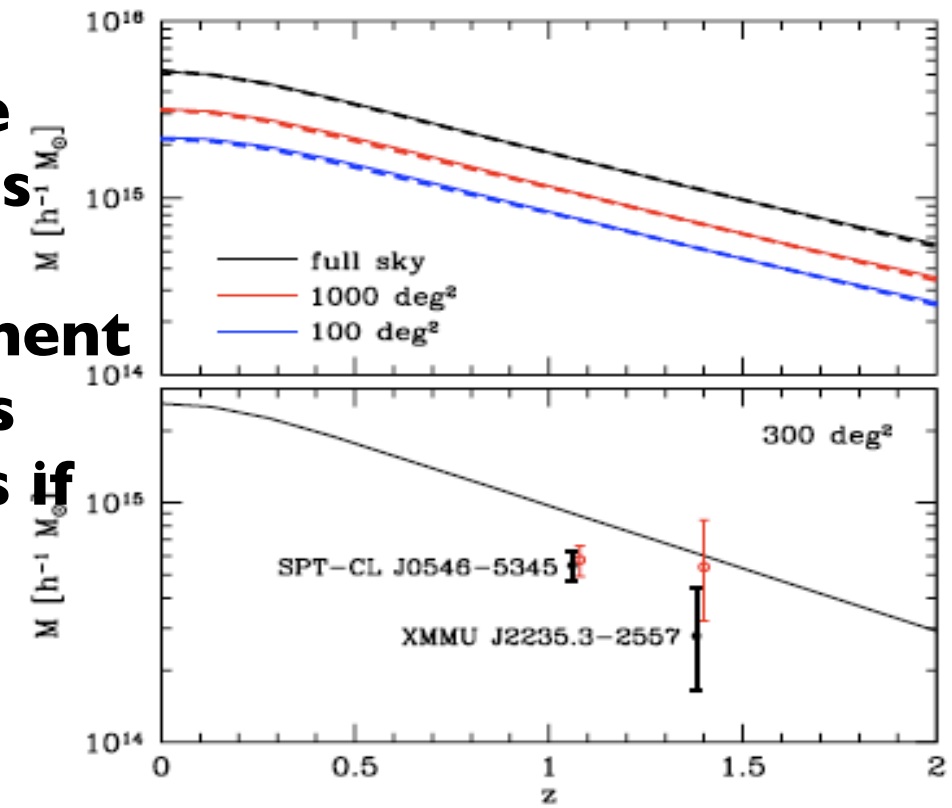


FIG. 4. $M(z)$ exclusion curves. Even a single cluster with (M, z) lying above the relevant curve would rule out both Λ CDM and quintessence. *Upper panel:* flat Λ CDM 95% joint CL for both sample variance and parameter variance for various choices of sky fraction f_{sky} from the MCMC analysis (thin solid curves) and using the fitting formula from Appendix A (thick dashed curves; accuracy to $\lesssim 5\%$ in mass). *Lower panel:* Two of the most anomalous clusters detected to date, compared with the 95% joint CL exclusion curve for 300 deg^2 which approximates the total survey area for each cluster. We show the X-ray determined masses with and without Eddington bias correction (black solid points with thin error bars and red open points with thin error bars, respectively offset in redshift by ± 0.01 for clarity).

Related works

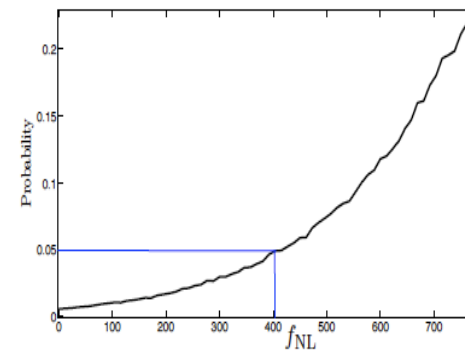
Mortonson et al 2010

- Treatment of the Eddington bias
- Tension curve for Λ cluster.

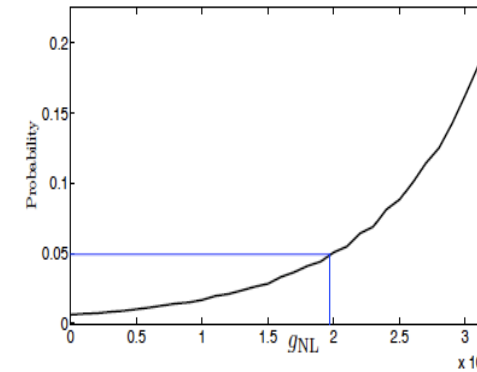
Enqvist et al 2010

- Agreed with us!
- Breakdown of the mass function
- Small f_{NL} , consistent g_{NL}

- Very conservative footprints and mass estimates.
- Insensitive treatment of multiple clusters
- Caution using this if know SF.

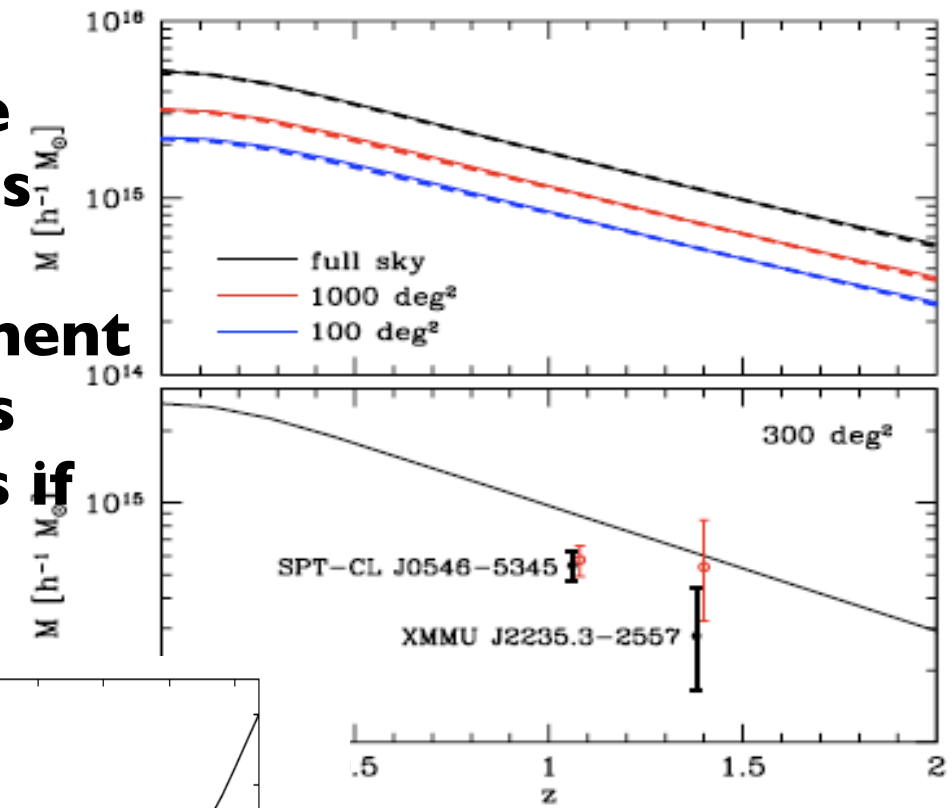


(a) The probability that the ensemble of clusters in table 1 could exist as a function of f_{NL} .



(b) The probability that the ensemble of clusters in table 1 could exist as a function of g_{NL} , with $f_{NL} \lesssim 50$.

Figure 6. Estimates for f_{NL} and g_{NL} .



curves. Even a single cluster with (M, z) curve would rule out both Λ CDM and Λ CDM: flat Λ CDM 95% joint CL for both f_{NL} and g_{NL} for a cluster variance for various choices of σ_8 . **Appendix A** (thick dashed curves; see **Appendix A** for details). **Lower panel:** Two of the most anomalous clusters, compared with the 95% joint CL excluding the total survey area. We show the X-ray determined masses with and without Eddington bias correction (black solid points with thin error bars and red open points with thin error bars, respectively, offset in redshift by ± 0.01 for clarity).

Related works

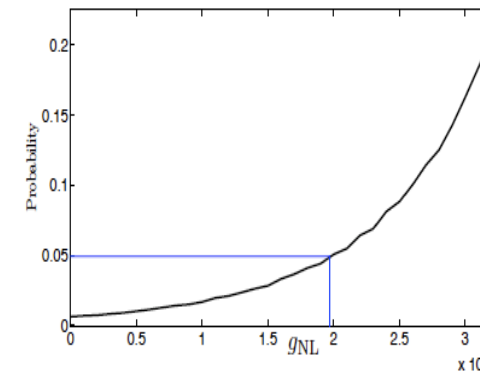
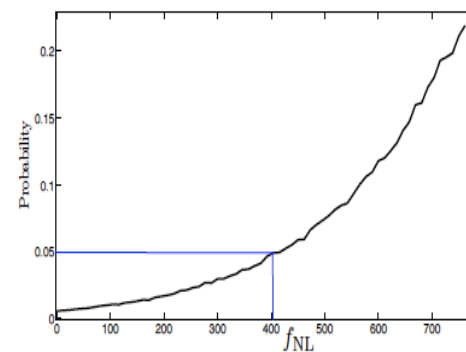
Mortonson et al 2010

- Treatment of the Eddington bias
- Tension curve for 1 cluster.

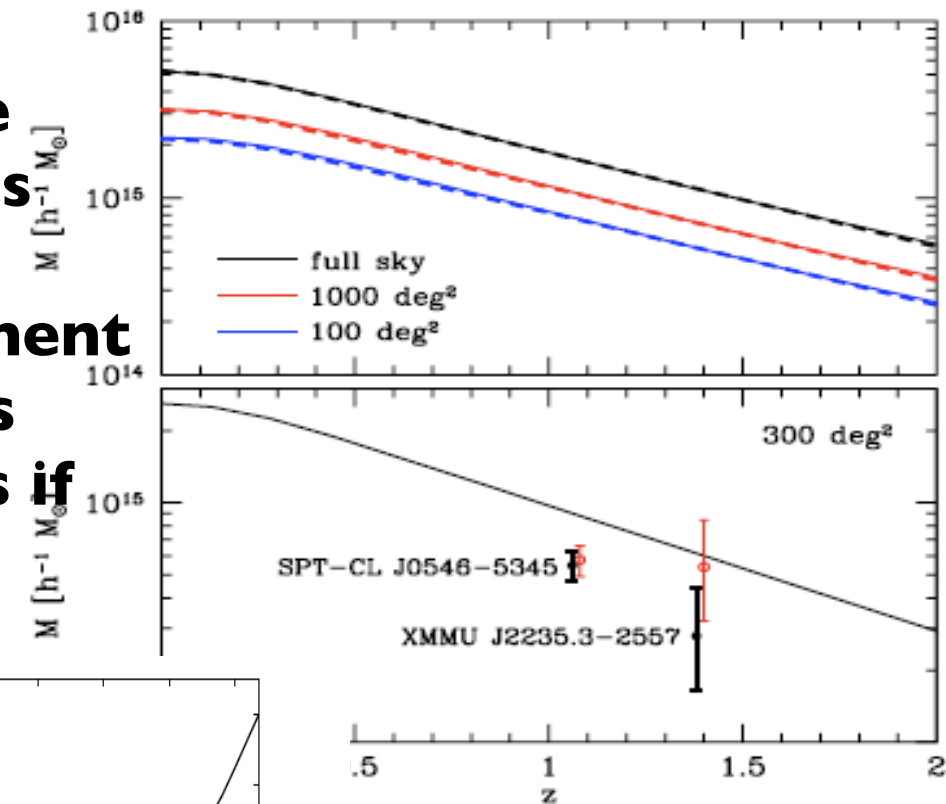
- Very conservative footprints and mass estimates.
- Insensitive treatment of multiple clusters
- Caution using this if know SF.

Enqvist et al 2010

- Agreed with us!
- Breakdown of the mass function
- Small f_{NL} , consistent g_{NL}



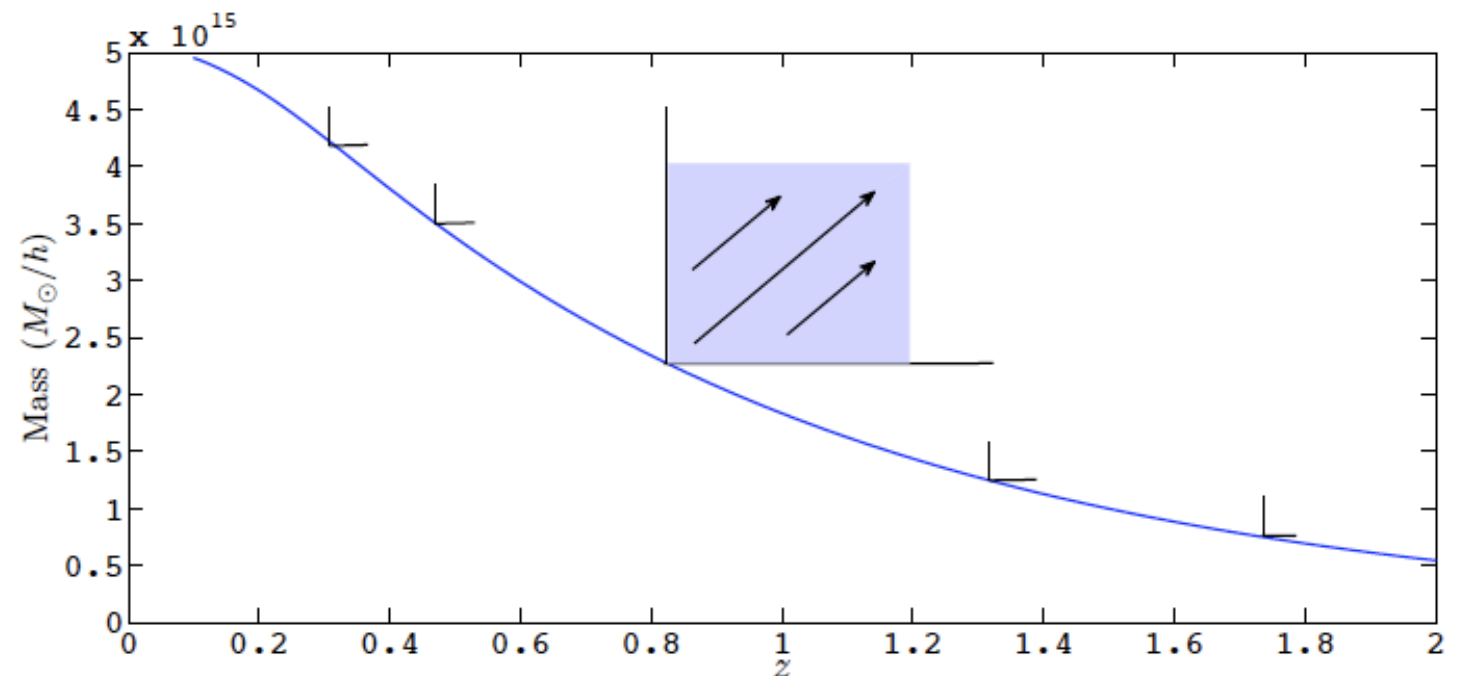
(a) The probability that the ensemble of clusters in table 1 could exist as a function of f_{NL} . (b) The probability that the ensemble of clusters in table 1 could exist as a function of g_{NL} , with $f_{NL} \lesssim 50$.



curves. Even a single cluster with (M, z) curve would rule out both Λ CDM and f_{NL} : flat Λ CDM 95% joint CL for both σ_8 and f_{NL} for various choices of σ_8 . Appendix A (thick dashed curves; see lower panel): Two of the most anomalous

Hotchkiss arXiv: 2011

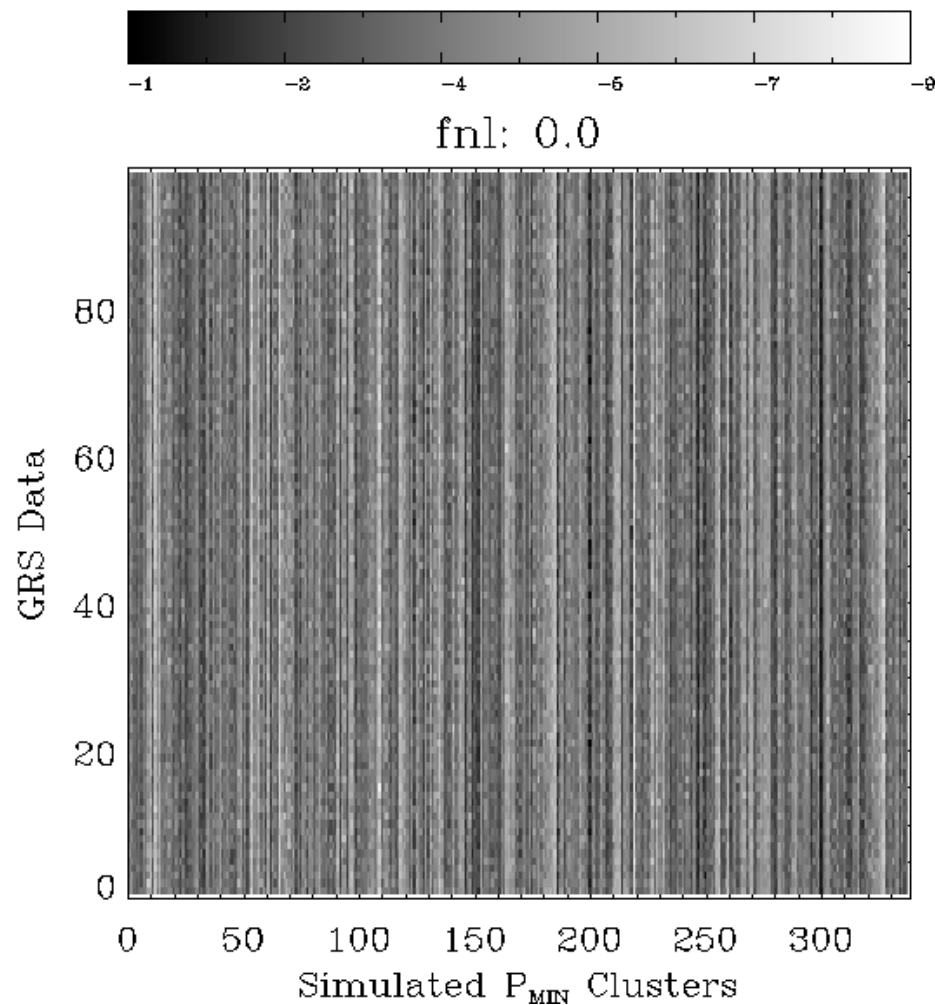
- Higher probability, but assumed the selection function was known. Integrated above the curve.
- If the observed clusters were consistent with being the Least Probable clusters, \rightarrow no tension with WMAP7 LCDM.
- If observed clusters random selection \rightarrow still caused tension.



Analysis & Results II

Comparing the clusters with the LP simulated clusters: 2d K-S test.

The 2d KS test determines if two 2d data sets are drawn from the same parent population. We Poisson sample from the theoretical mass function, and compare the resulting distribution in the (M,z) plane of the LP clusters from each simulation with each other (varying WMAP7 cosmology) and with the data.



Results

- **The simulated LP clusters are consistent with each other ($P=0.2$)**
- **The simulated LP clusters are not consistent with the data ($P=0.001$).**

-> Tension with LCDM still remains.

Conclusions/Future work

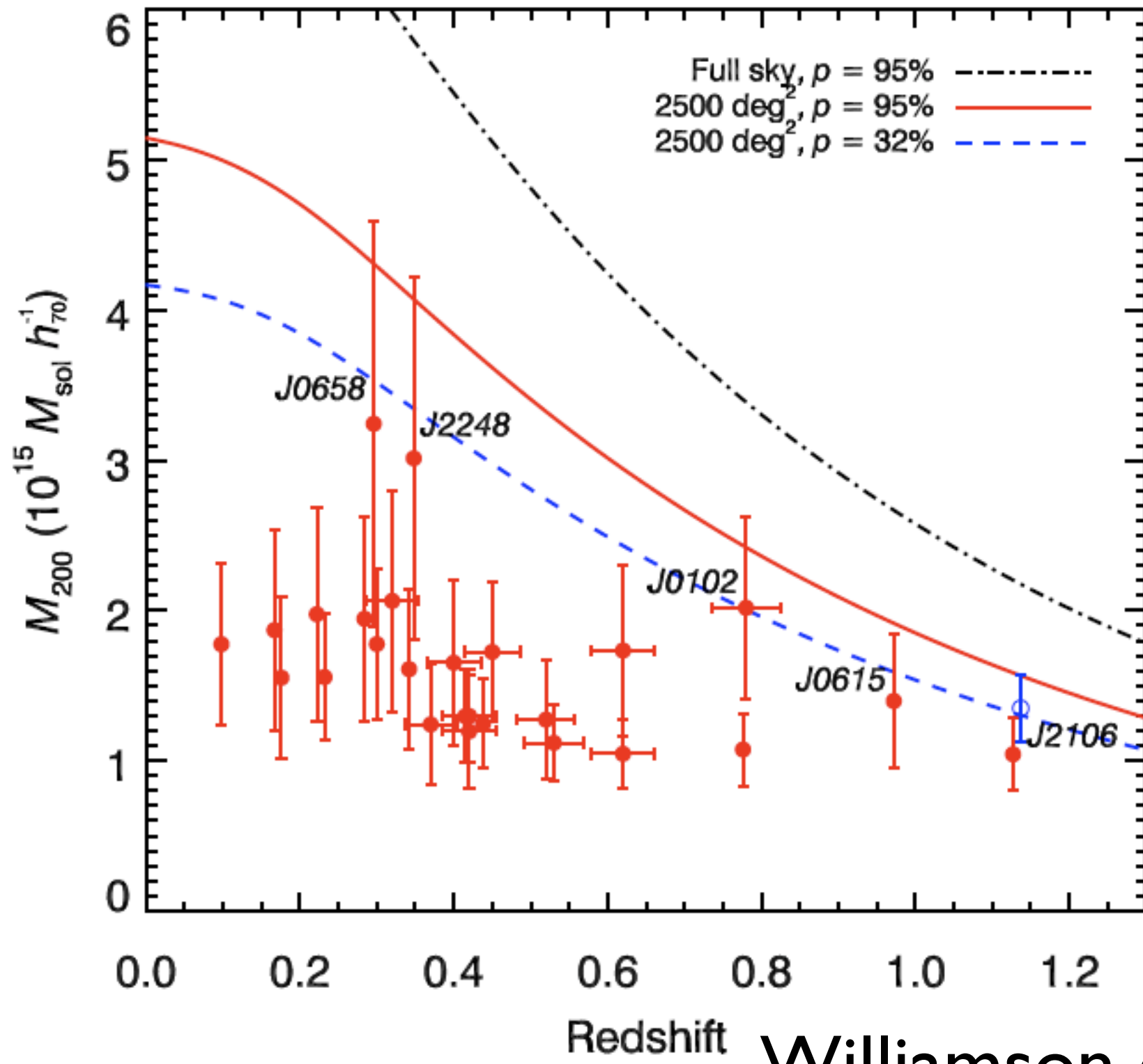
These clusters still pose a question to LCDM with WMAP priors on cosmological parameters.

$$\sigma_8 = 0.9 \quad \text{or} \quad M_{TRUE} = M_{OBS} - 1.5 \times \Delta M \quad \text{or} \quad f_{NL}|_{P(0.05)} \gtrsim 123 \text{ at the 95\%}$$

or **mass function uncertainty.**

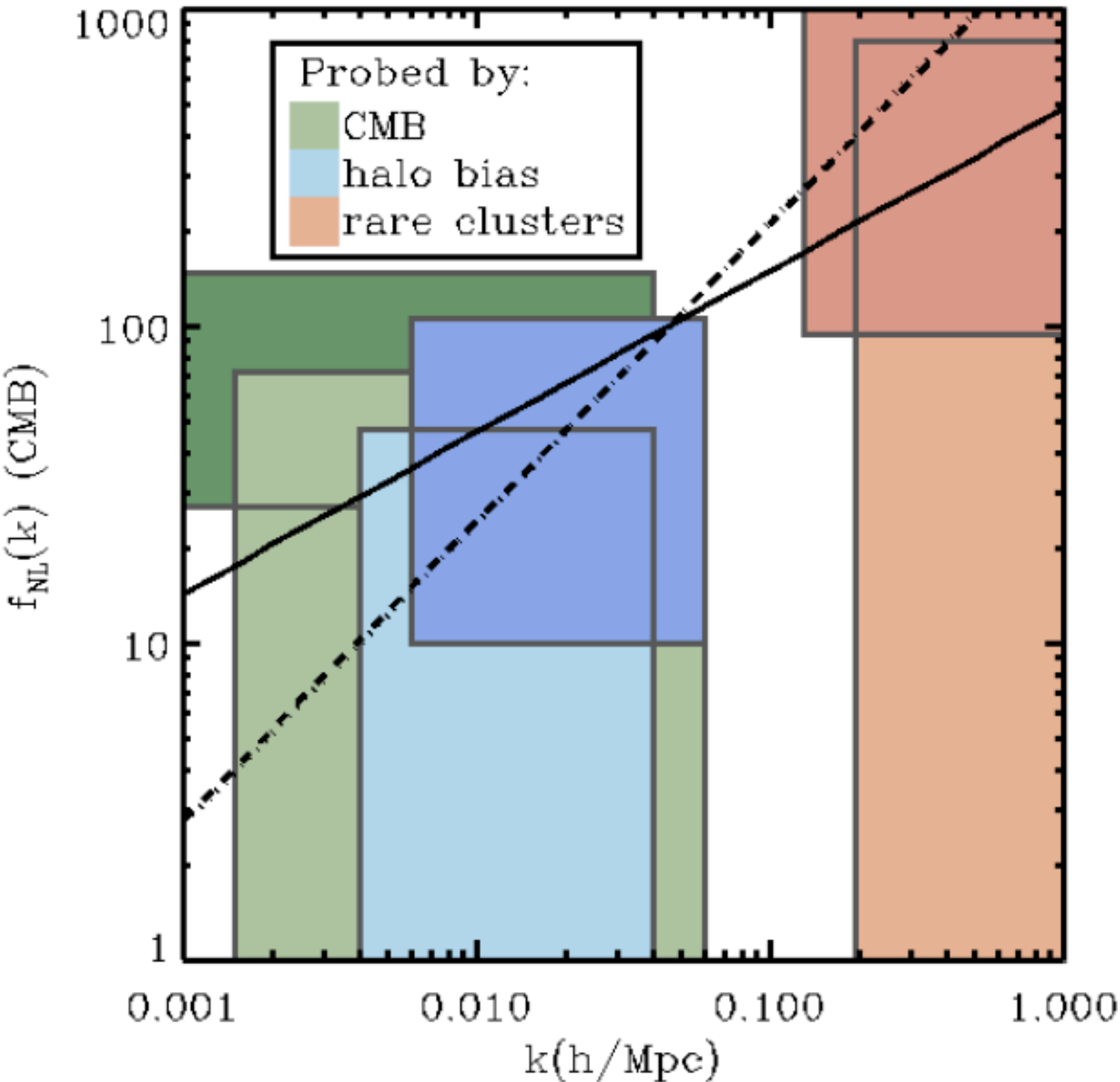
- **Built a list of high redshift clusters.**
- **Conservative footprint/survey/completeness/mass assumptions.**
- **Attempted to quantify the tension with LCDM.**
- **Showed how fnl or systematics can reduce tension, and work to reduce systematics.**
- **No consensus as to the level of tension, or how to quantify it.**
- **A more rigorous approach to quantifying tension and parameter estimation is developed in Hoyle et al (in prep)**

• **But, more high redshift, massive clusters are being found ~weekly. SPT release/Planck /XCS, so we need a framework to understand what they tell us about LCDM**



Williamson et al 2011

If f_{NL}, then Scale Dependent non-Gaussianity



WMAP CMB, scales 0.04 h/Mpc

$27 < f_{NL} < 147$, at the 95%

Yadev & Wandelt 2008

$f_{NL} = 32 \pm 21$ at 1σ

Komatsu et al 2011

Halo bias, scales 0.1 h/Mpc

$10 < f_{NL} < 106$ at the 95%

Xia et al 2010

$-77 < f_{NL} < 47$ at the 95%

Slozar et al 2008

Galaxy Clusters, scales 0.4 h/Mpc

449 ± 286 at 1σ

Cayon et al 2010

$f_{NL}^{LSS}|_{P(0.05)} \gtrsim 123$ at the 95%

Hoyle et al 2010

$$f_{NL} = f_{NL}^* \left(\frac{k}{k^*} \right)^{n_{NG}} \quad n_{NG} = 0.50 \pm 0.19 \quad n_{NG} = 0.95 \pm 0.23$$

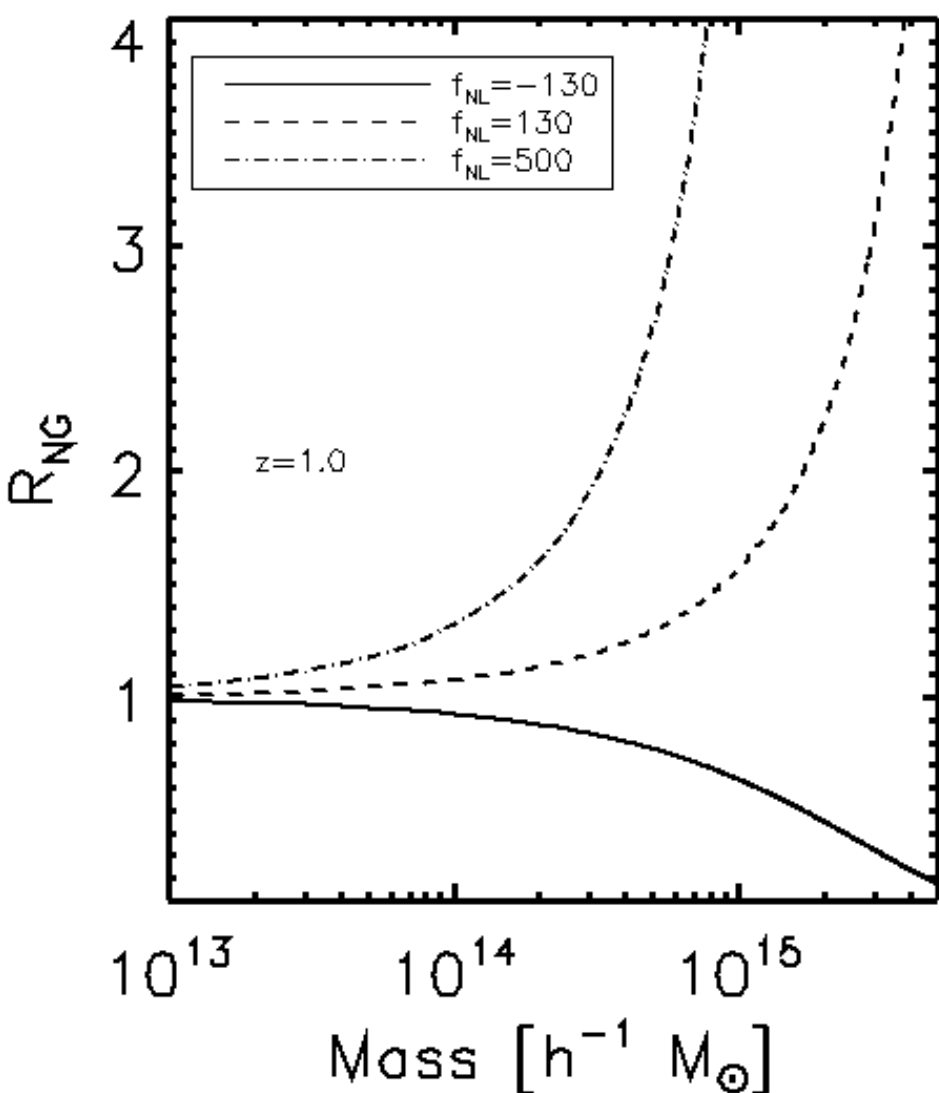
Lo Verde et al 2008

Modifying the mass function with non-Gaussianity

We can change the number of expected clusters by allowing some f_{NL} which modifies the cluster mass function.

$$n_G(M, z) = \sqrt{\frac{2}{\pi}} \frac{\bar{\rho}}{M^2} \left| \frac{d}{d \ln M} \ln \sigma_M \right| \nu \exp -\nu^2/2. \quad \mathcal{R}_{NG}(S_{3,M}, M, z) = \frac{n(M, z, f_{NL})}{n_G(M, z, f_{NL} = 0)}$$

Solved in the Press-Schechter type formalism by Matarrese, Verde, Jimenez 2002, LoVerde et al 2007, Maggiore et al 2009, D'Amico et al 2010 etc.



$$\mathcal{R}_{NG}(M, z, f_{NL}) = \exp \left[\delta_{ec}^3 \frac{S_{3,M}}{6\sigma_M^2} \right] \times$$

$$\left| \frac{1}{6} \frac{\delta_{ec}}{\sqrt{1 - \frac{\delta_{ec} S_{3,M}}{3}}} \frac{dS_{3,M}}{d \ln \sigma_M} + \sqrt{1 - \frac{\delta_{ec} S_{3,M}}{3}} \right|,$$

The normalised skewness of the smoothed density field

$$S_{3,M} = f_{NL} S_{3,M}^{f_{NL}=1}$$

Rng enable other, better calibrated mass functions to be used (e.g., Jenkins et al 2000, Tinker et al 2008, Wagner et al 2010).

Motivation: theory, a window to the early Universe

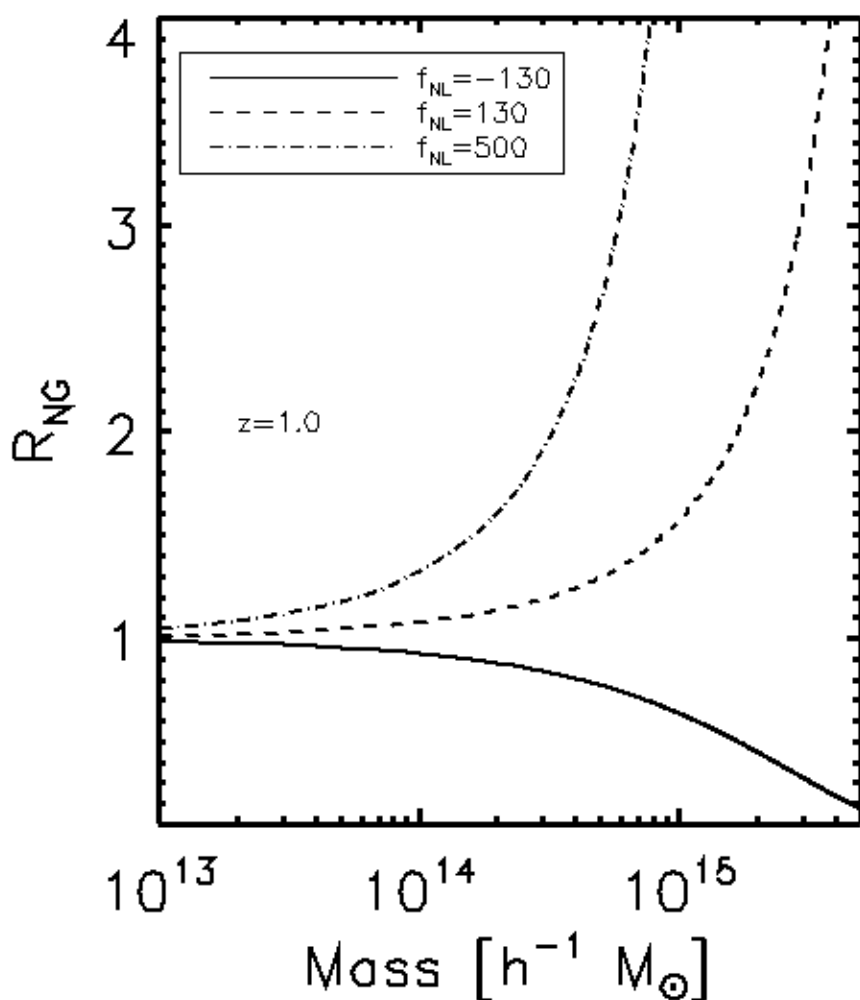
Using today's data, (not some future experiment e.g. LISA-like) we can make a measurement of the primordial non-Gaussianity (f_{NL}) which can tell us about the various types of scalar field interactions during inflation/reheating/preheating.

$$\Phi = \phi + f_{\text{NL}} (\phi^2 - \langle \phi^2 \rangle) .$$

Hand wavy theory for observers

Within the (perturbed) lagrangian for the scalar fields in the early universe:

$$\Pi^3, (\partial\Pi)^3, \Pi(\partial\Pi)^2, \Pi_1\Pi_2\Pi_1 \rightarrow f_{\text{NL}}(k)(n_{\text{NG}}) \sim ?$$



A single, multiply coupled field or two (or more) couple fields generate the bispectrum and can produce large non-Gaussianities (skewness) with scale dependence. e.g., Byrnes et al 2010 [arXiv:1007.4277]

$$n_G(M, z) = \sqrt{\frac{2}{\pi}} \frac{\bar{\rho}}{M^2} \left| \frac{d}{d \ln M} \ln \sigma_M \right| \nu \exp -\nu^2/2 .$$

$$\mathcal{R}_{\text{NG}}(S_{3,M}, M, z) = \frac{n(M, z, f_{\text{NL}})}{n_G(M, z, f_{\text{NL}} = 0)}$$

XCS:

Current X-Ray Cluster Surveys



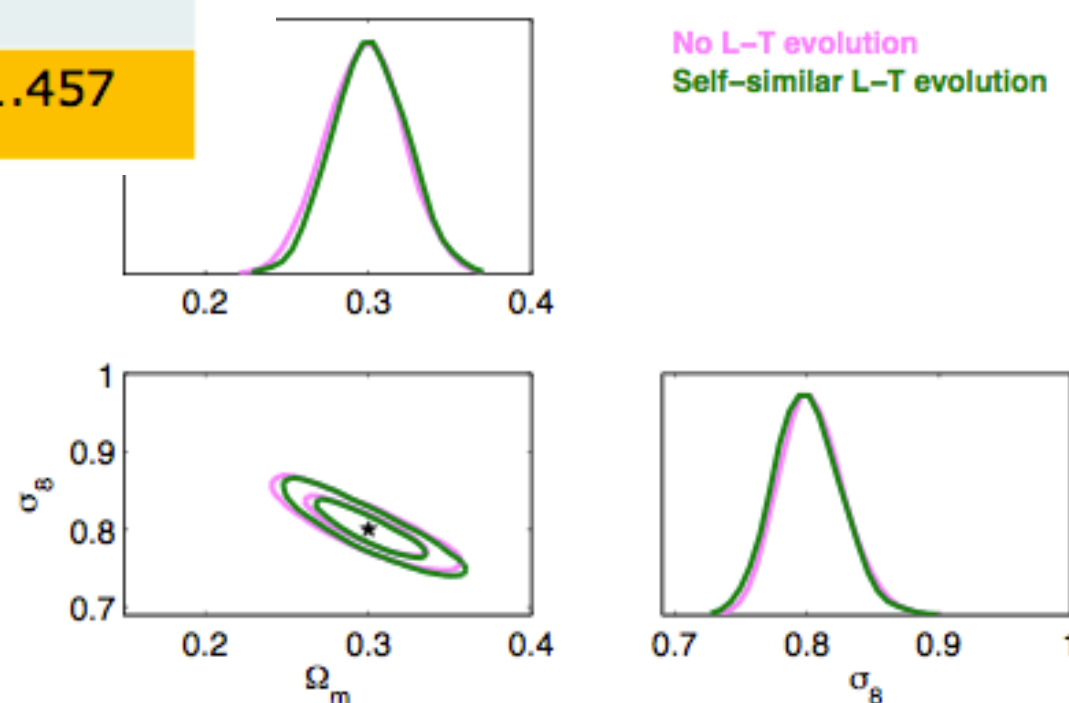
Survey	Data	Clusters	Redshift range
HIFLUGCS	ROSAT	63	0.005 – 0.2
Maughan et al.	Chandra	115	0.1 – 1.3
O'Hara et al.	Chandra	70	0.18 – 1.24
400d	ROSAT/Chandra	86	0.35 – 0.9
XMM-LSS	XMM	29	0.05 – 1.05
Mantz et al.	ROSAT/Chandra	238	0.05 – 0.45
Peterson et al.	Chandra/XMM	723	0 – 1 ?
XCS₃₀₀ (230 °)	XMM	450	0.003 – 1.457

**Forecast papers:
Cosmological constraints**

Martin Sahlen et al 2009, and in prep.

**503 clusters, spanning $0.06 < z < 1.46$
438 have x-ray temperatures**

Data release, Mehrtens et al. in prep (very soon!)

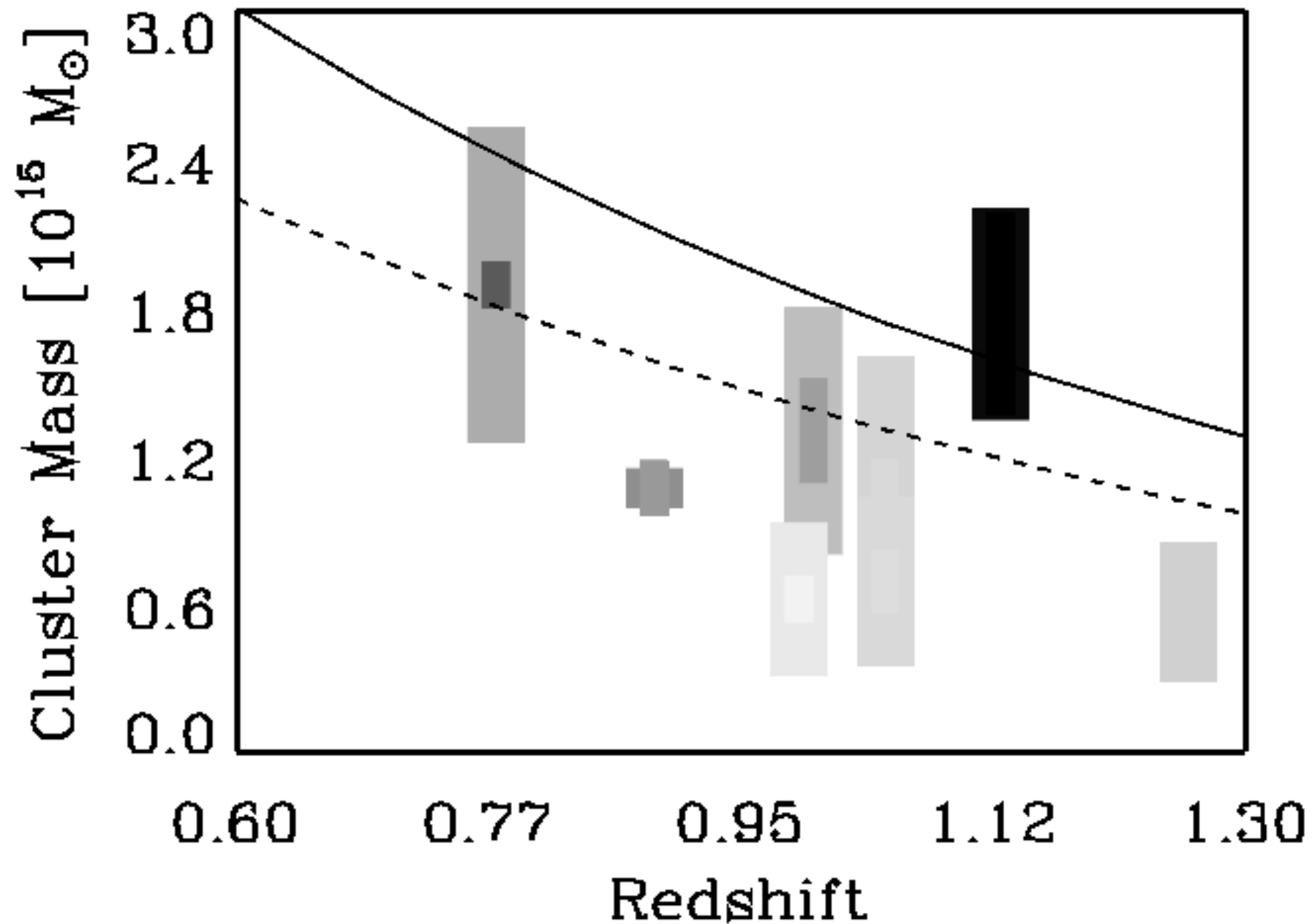


HST proposal

Mortonson et al type exclusion curves, and the change in Probability of existence with HST WL mass estimates assuming the peak mass value is unchanged.



← Prob(\exists)=3.0% Prob(\exists)=77% →



XCS:

Optical Followup

Purity with Cluster Zoo

All clusters multiply classified by experts to determine purity.

IUG, University of Portsmouth.

XCS XCS extended source identification **SDSS**

Hello Kath! Click here to [Log out](#)

XCS classification page

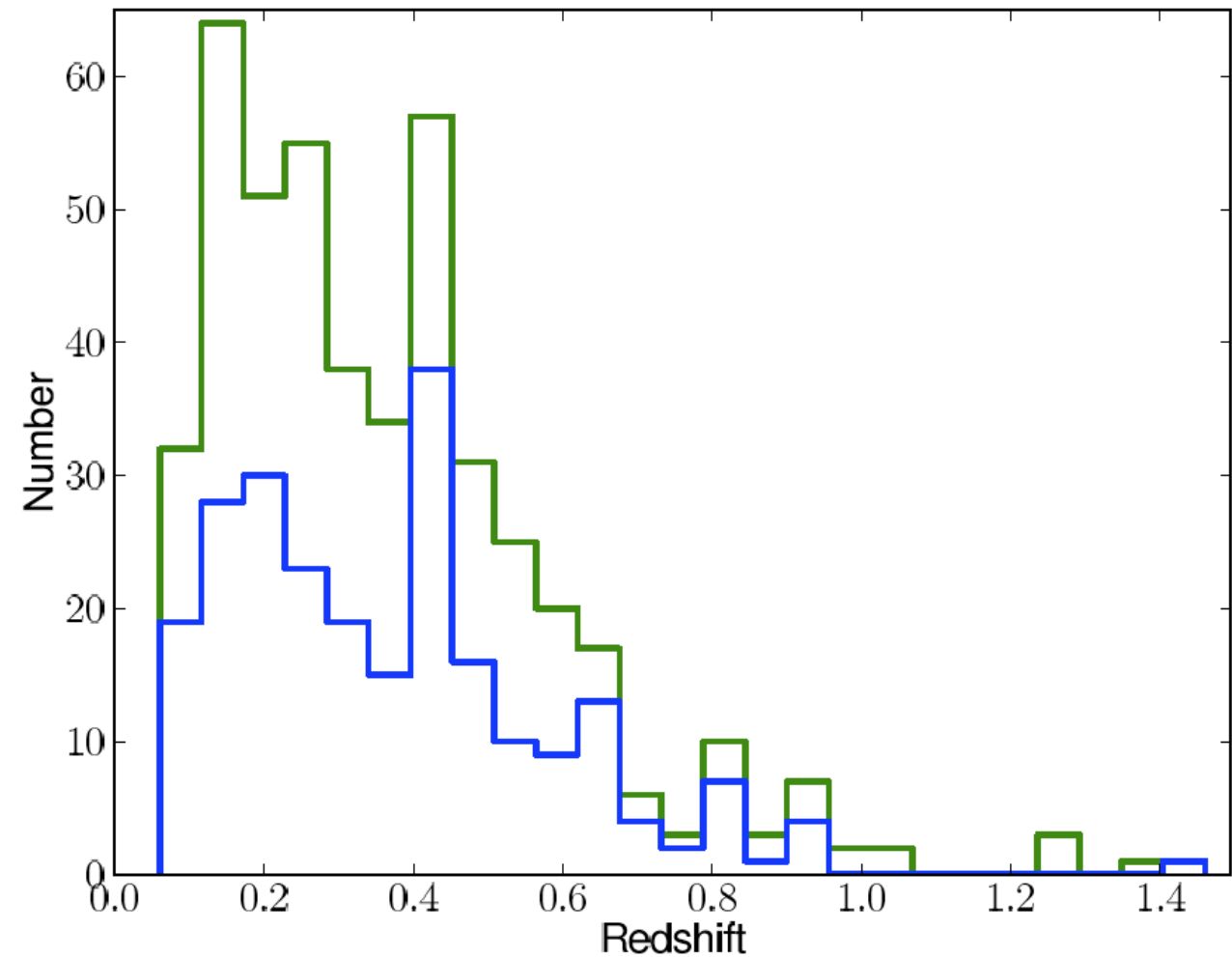
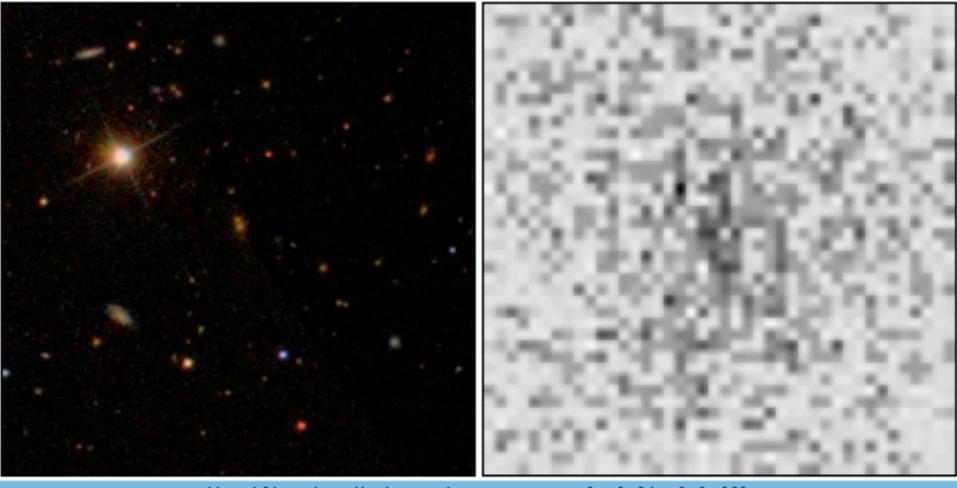
Please examine the figures found under the Optical&X-ray images and Raw data tabs, before making an extended source classification decision, under the third tab. This session you have made 0 classifications. Your target is 30. Access the [classifications here](#)

[Optical&X-ray images](#) [Mask data](#) [Make your classification](#)

Optical and Xray images

Scrolling down the page displays images of the extended sources to be classified at three magnifications in the optical and x-ray. Simply moving (no need to click) your mouse over the contours: [\[on\]](#) and [\[off\]](#) links show and hide the contours, while [\[inv\]](#) inverts the sdss image, and highlights photometric objects. Don't like this cluster [Skip it here](#).

Magnification 3by3 zooms contours: [\[on\]](#) [\[inv\]](#) [\[off\]](#)



503 clusters, spanning $0.06 < z < 1.46$
438 have x-ray temperatures

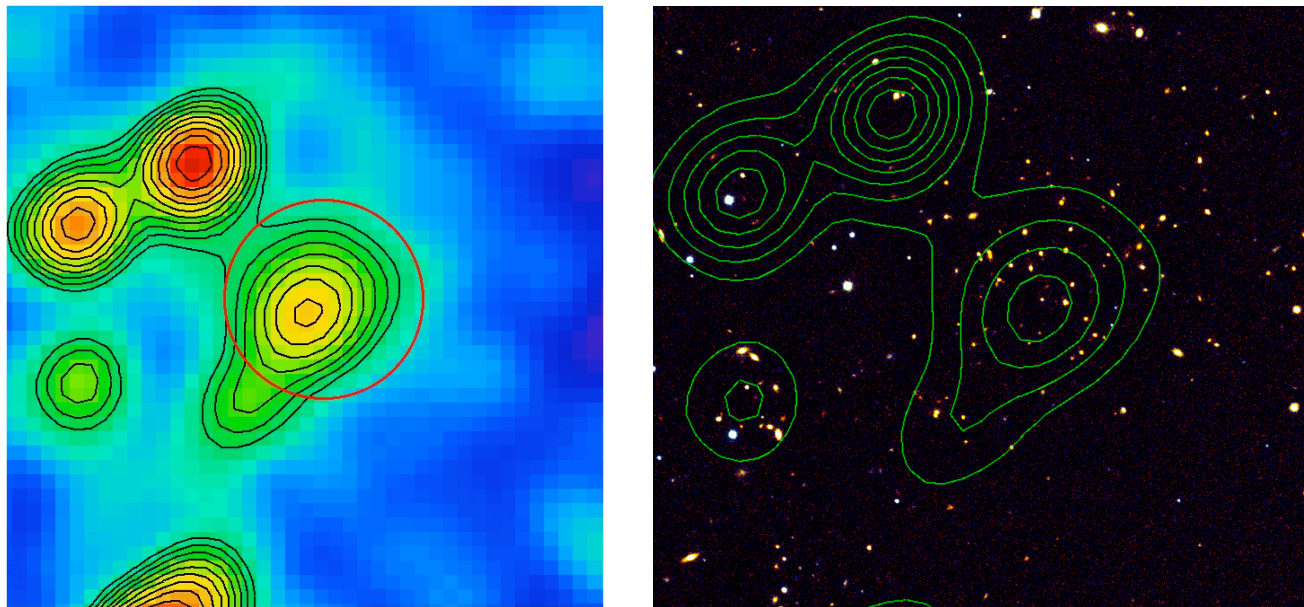
Recent data release, Mehrrens et al. arXiv:1106.3056

XCS:

Other results.

XMMXCS J2215

Was the highest redshift X-ray selected cluster, $z=1.46$ (Stanford et al. 2006, Hilton et al. 2007, 2008)

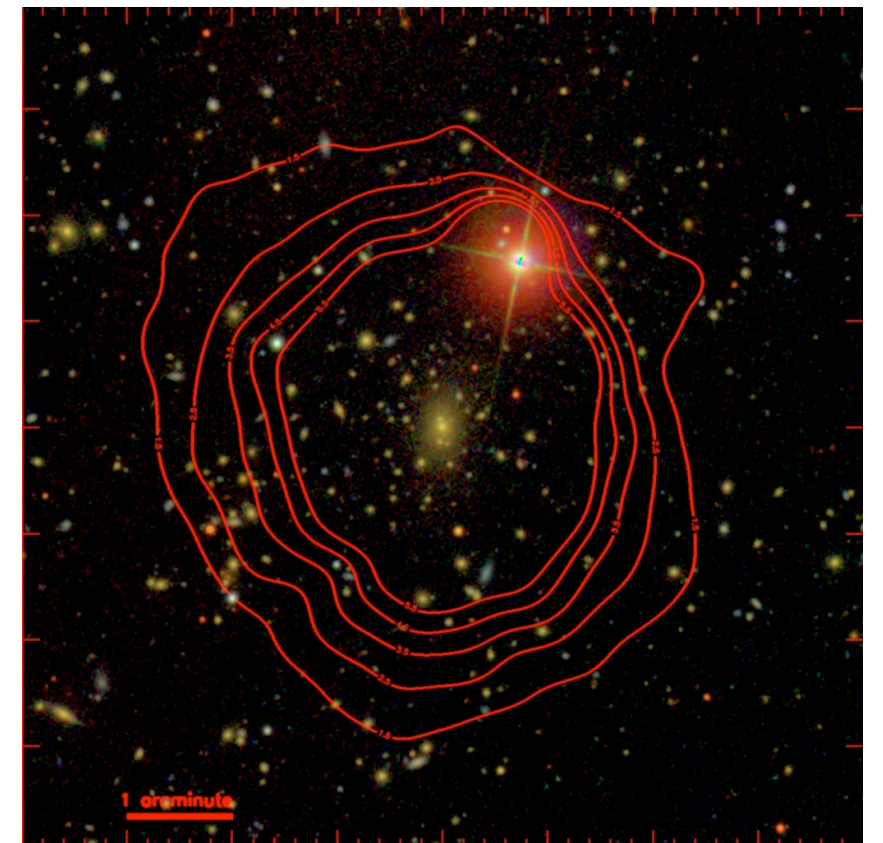


Now $z=2.07$, $M \sim 5-8 \cdot 10^{13} \text{ SolMass}$,
Gobat et al arXiv:1011.1837

503 clusters, spanning $0.06 < z < 1.46$
438 have x-ray temperatures

Recent Data release, Mehrtens et al. arXiv:1106.3056

Fossil groups



- 15 Fossil Groups
- $z < 0.25$
- 0.9-6.6 keV
- Galaxy evolution

Harrison et al
(submitted)